

A COMPUTATIONAL STUDY FOR A WING AT OR PITCHING UP TO HIGH ANGLE OF ATTACK IN PRESENCE OF A SPANWISE GUST

Batuhan EROĞLU¹, Berk ZALOĞLU², Okşan ÇETİNER³
Istanbul Technical University
Istanbul, Turkey

Arif Cem GÖZÜKARA⁴
ASELSAN
Ankara, Turkey

ABSTRACT

Two cases involving massive flow separation have been studied numerically in presence of a spanwise gust. A NACA0012 wing has an aspect ratio of 4 and is either at an angle of attack of 45° or pitching up from zero to the same angle of attack in a uniform flow of $Re=10000$. Previous numerical studies in the absence of gust showed good agreement with the experimental studies and the current investigation aims to simulate those two cases when the incoming flow has a large scale sinusoidal transverse fluctuations and compare with available equivalent experimental results.

INTRODUCTION

Gust effects on Micro Air Vehicles (MAV) have been investigated through numerical and experimental methods. Since the MAV aerodynamic load generation and gust effects are results of low aspect ratio wings in low Reynolds numbers, researchers have managed to recreate the motions of structures and fluid flows in water channels, wind tunnels and computational domains. Both methods of research have drawbacks and aspects where they are superior to one another. Although experimental methods are much more reliable, they are expensive and require high precision sensors. They are also insufficient in capturing every aspect of a case. On the other hand, numerical methods are dependent on meshing quality, are less reliable than well-conducted experiments and limited by the computational power available. However, they can lay out the entire characteristics of a case and they are highly reproducible.

Understanding and replicating the exact conditions a MAV will endure is critical for accurate, comprehensive understanding of MAV dynamical behavior. MAV mission requirements demand the aircraft to be immersed in the lower atmosphere where the flow can be highly turbulent. This turbulent zone called the Atmospheric Boundary Layer (ABL) acts much like a boundary layer, extending from the Earth's surface to between 100 m to 1000m, depending on the terrain and climate conditions [Watkins et al, 2006].

¹ Graduate student in Aeronautical and Astronautical Engineering Department, Email: eroglu@itu.edu.tr

² Graduate student in Aeronautical and Astronautical Engineering Department, Email: zaloglu@itu.edu.tr

³ Professor in Astronautical Engineering Department, Email: cetiner@itu.edu.tr

⁴ Lead Engineer, Email: cgozucar@aselsan.com.tr

There has been numerous investigations of the lower atmospheric layer by different scientific communities. Watkins et al. [Watkins et al, 2006] argued that these data were not applicable to MAV applications due to lack of resolution, hence they acquired turbulence data from probes mounted on a moving car. Their results showed an increase in turbulence intensity from %4 to %40, with decreasing velocity. Further data has been published by Milbank et al. [Milbank et al, 2005].

Experimental researchers have worked on creating controllable turbulent flows by active and passive methods to create ABL conditions for various cases [Fisher, 2013]. Kang et al. [Kang et al, 2003] used active grids with winglets connected to motors to create desired turbulence, Comte-Bellot and Corrsin [Comte-Bellot and Corrsin, 1966] placed different shaped grids and measured the turbulence characteristics downstream.

Lian and Shyy [Lian and Shyy, 2007] numerically investigated gust effects on a pitching and plunging NACA 0012 airfoil. They examined the pitching plunging wing at $Re=40000$ and 4° of angle of attack in a head on gust with a frequency of 1 Hz. Results showed that the time averaged thrust coefficient varied very little in contrast to the freestream variation due to gust. Hence, they concluded that pitching and plunging motion at certain amplitudes and frequencies act in a way that stabilizes thrust generation. Lian [Lian,2009] numerically studied a pitching and plunging airfoil under different gust amplitude, frequencies and kinematic patterns. He measured basic forces and performance coefficients for different cases. Results show that certain kinematic patterns and pitching and plunging frequency and amplitude result in better gust resistance.

This study aims to investigate numerically a massively separation case in presence of a spanwise gust with a wing either at an angle of attack of 45° or pitching up to 45° and tune the solution based on the available experimental data. The gust characterization and those test cases are experimentally available in terms of quantitative flow visualization via DPIV (Digital Particle Image Velocimetry) data and simultaneous force measurements.

METHOD

The numerical computations were performed by using the commercial software package ANSYS Fluent 15.0 [ANSYS® Fluent, 2013a and ANSYS® Fluent, 2013b]. NACA 0012 wing with an aspect ratio of 4 and chord length of 0.1 m had been used in the numerical computations. The fluid density and viscosity are assumed to be constant and SIMPLE method [Patankar and Spalding, 1972] had been used for pressure-velocity coupling in both computational case. The governing equations used in the simulations are unsteady, incompressible, 3D Navier-Stokes equations [Anderson, 1995]. Spatial discretization is made by using second order upwind-type schemes and the temporal discretization is made by using a second order scheme. The time step size is chosen accordingly, to satisfy the residual convergence on the order of 10^{-4} . In the computations, one convective time which corresponds to one chord of travel and equal to 1 second, is divided into 500 equal time steps.

The first computations are performed to simulate the presence of a spanwise gust while the wing is at a 45° angle of attack. The flow domain of this computations is constructed as a 26 c long, 24 c wide and 20 c high prismatic volume in order to replicate the experimental setup of the free-surface water channel located at Trisonic Laboratory, ITU.

The wing is positioned in the computational volume 10 chords away from side walls and 5 and 20 chords away from inlet and outlet boundaries respectively. The mesh size and density in the vicinity of the wing had been controlled by constructing an inner bell shaped volume around the wing. A general view of the flow domain that is used in computations of both cases can be seen in Figure 1.

The mesh, which had been used in these computations is obtained as a result of mesh independence study. The final mesh used in contains 19897389 tetrahedral elements. In this URANS simulation k- ϵ Realizable [ANSYS® Fluent, 2013b] model had been used for the turbulence closure.

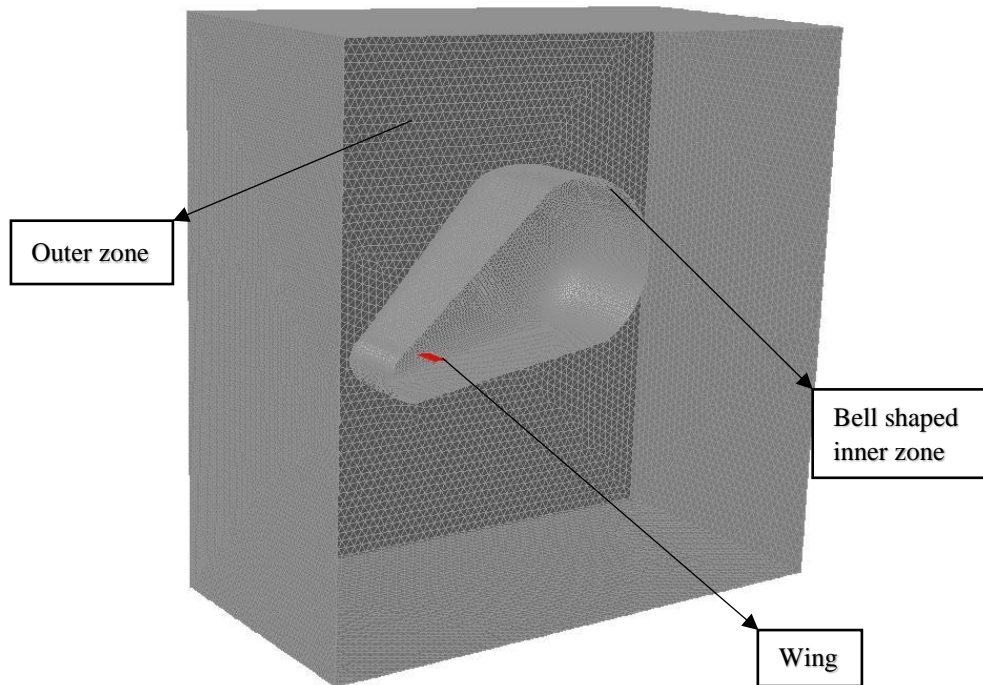


Figure 1: Computational flow domain structure

Second part of computations had been performed for simulating the wing, pitching up to 45° angle of attack in presence of a spanwise gust. In the pitch-up case, moving-deforming mesh feature of the software is used for implementation of the motion kinematics. The computational domain is composed of two zones similar to the prior case. The outer grid zone surrounds a bell shaped inner zone. This inner mesh zone is moving with the wing without going through a deformation. The mesh density and quality is kept constant around the wing by the rigid body motion of the inner grid zone. The outer grid zone is morphed and regenerated according to the predefined deformation rules to enable inner zone to move [Stevens et al, 2016].

The computational grid used in the pitch-up case simulations are composed of 17032596 tetrahedral elements. In the grid, prismatic elements are used in the vicinity of the wing for increasing the resolution and mesh quality. The grid independence is tested by performing steady state computations at different incidence angles with different number of elements.

The computational domain used in these simulations is a 35 c long, 35 c wide and 35 c high cubic volume. In the URANS simulation of pitch-up case $k-\omega$ SST [ANSYS® Fluent, 2013b] model had been used for the turbulence closure.

In a previous study, periodic vortex gusts are generated in the water channel [Biler et al., 2015]. The spectral analysis of the velocity field in the wake of the oscillating plate were used to characterize the gust. Three different gust types with varying frequencies and amplitudes have been obtained and identified such that all can be considered as spanwise gusts where the streamwise fluctuations are minimized.

The pitching NACA0012 airfoil was subjected to these three gust types, as given in Table 1. In addition to the gust cases, No Gust case was also investigated. On the other hand, the model were subjected to perform two types of motion: fast pitch-up and slow pitch-up. The model started from 0° and attained its final angle of attack of 45° in 1 second for the fast pitch-up motion and in 6 seconds for the slow pitch-up motion; corresponding to 1 and 6 convective times, respectively. Four gust encounter times have been studied; the pitch-up motion is synchronized with the gust generator plate with phase angles of $\phi = 0^\circ, 90^\circ, 180^\circ$ and 270° .

The computational simulations take only into account Gust No 3 for the wing undergoing fast pitch-up motion.

Table 1: *Gust parameters*

Gust No	Frequency [Hz]	Amplitude
1	0.5	0.9 U_∞
2	0.25	0.3 U_∞
3	0.25	0.9 U_∞

RESULTS

The first part of the study considers the wing at an angle of attack of 45° subject to Gust 3. Figure 2 shows the y -component velocity distribution and Figure 3 shows the lift coefficient variation in comparison with the experimental data. Although there are some differences in the experimental conditions, the computational results for the lift coefficient variation in a cycle of sinusoidal gust agree well with the experimental data. It should be noted that the wing aspect ratio is 6 with the use of an endplate in the experiments, on the other hand, the wing has an aspect ratio of 4 in the computations.

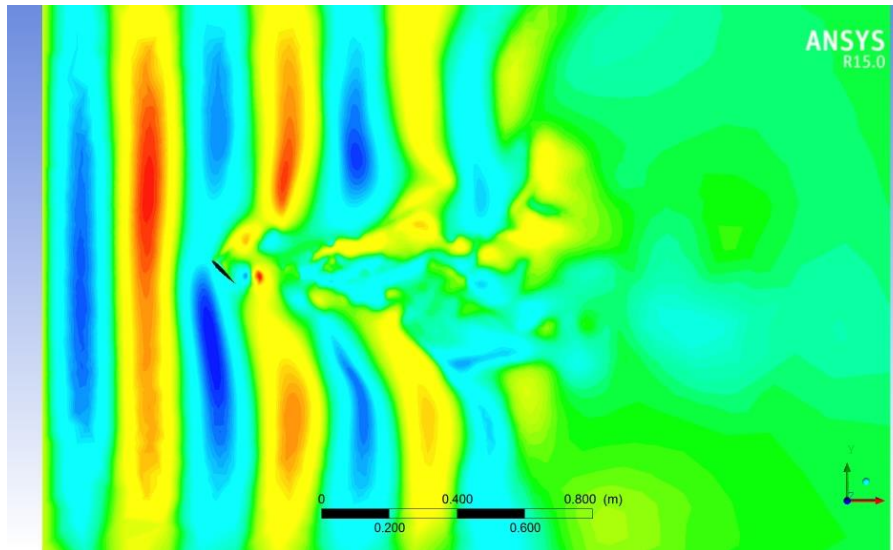


Figure 2: The gust fronts for the wing of AR=4 at an angle of attack of 45°

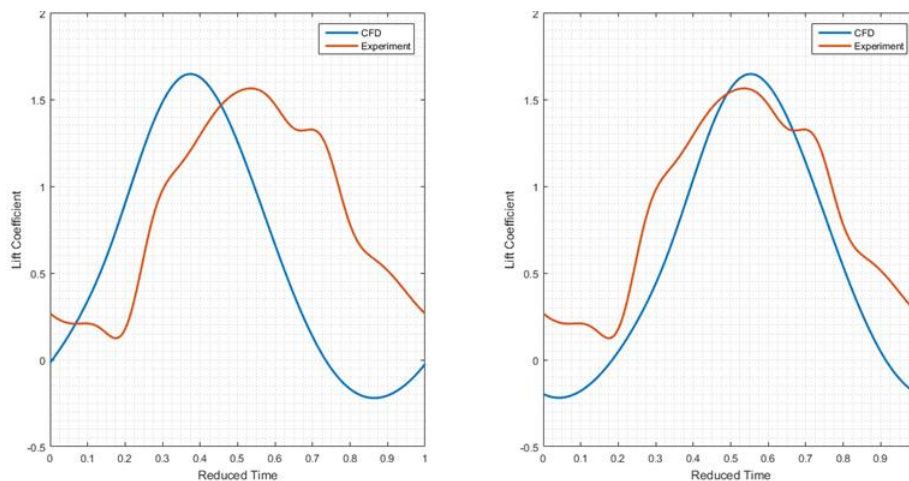


Figure 3: Comparison for computational and experimental lift coefficient variation; left: before adjusting the time axis, right: after adjusting the gust encounter timing.

The gust in consideration in the experiments has a frequency of $f=0.25\text{Hz}$ and has a peak amplitude of 0.09m/s which is 90% of the freestream velocity. On the other hand, the encounter time of the gust with respect to the wing pitch-up motion is determined based on the gust generator motion. The input to the simulations is given as considering the plane 50mm upstream of the leading edge, the sinusoidal variation (sinus function) starts at $t=4.5\text{s}$ and reaches maximum at $t=5.5\text{s}$, while the experiments consider a phase of 0° when the wing starts to pitch up $t=4\text{s}$. However, for the sake of simplicity, the simulations take into account sinusoidal (cosines function) variation at the leading edge plane and starting in phase with the pitch-up motion which starts at $t=6.2\text{s}$. Figure 4 shows the lift coefficient variation with time and only a difference of 2.2s is considered plotting the force coefficients in comparison. As noticed in the zoomed-in view the experimental data belonging to a phase variation of 180° matches the simulations. Indeed if we take into account the functions and the gust front convection at the freestream velocity, two considerations have a difference of 2s which is equivalent to a phase difference of 180° . Figure 4 also shows only the two variations along with the lift coefficient variation in the absence of gust in a zoomed-in view. Although there are some differences in the two considerations including the perfect transverse velocity variations without any fluctuations in the freestream direction and any allowed space for the wing motion to affect the upstream gust, the simulations match the major characteristics of the force variation.

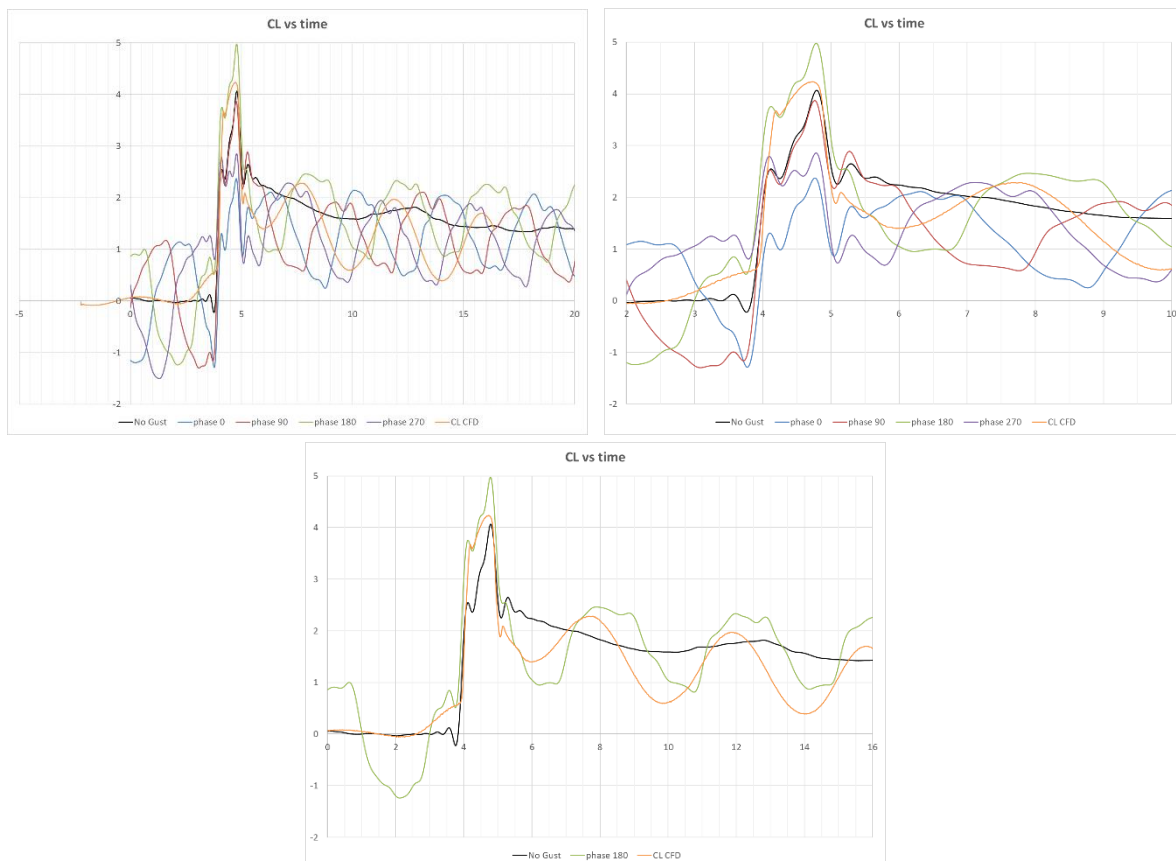


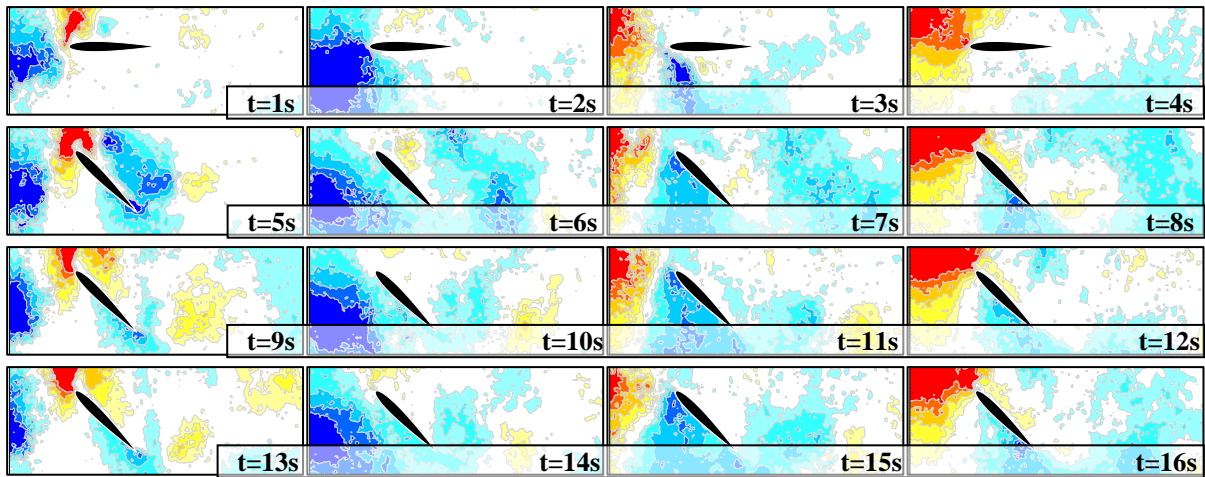
Figure 4: Experimental and computational lift coefficient variations of pitch-up case with time

The transverse velocity distributions are obtained experimentally and computationally, and plotted during four gust periods including the motion. Figure 5a shows the experimental DPIV results taken at the physical mid span which actually corresponds to the quarter span because of the use of an endplate which eliminates free-surface effects and acts as a symmetry plane. Previous work [Son and Cetiner, 2017; Son et al, 2016] showed that this plane of visualization is still far from the tip effects and gives a close result as that of the mid span for a wing of $AR=4$ undergoing same motion in the absence of a gust. The advantage of the computational

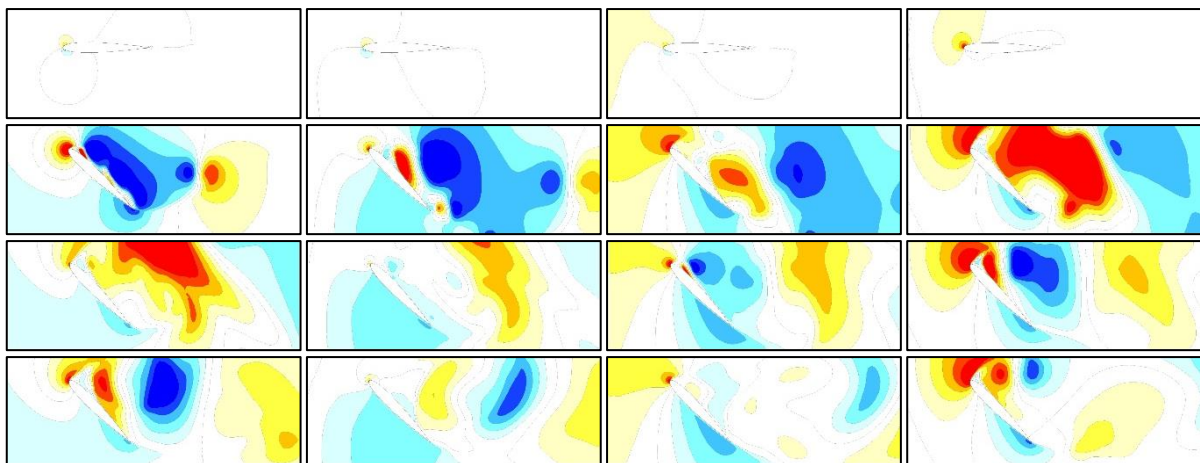
approach is to provide a full three-dimensional quantitative flow visualization. While Figure 5b matches the time of snapshots at the mid plane, Figure 5c visualize the transverse velocity distributions only for the last two periods of gust at the quarter span plane. The experimental results shows clearly the periodicity of the gust although the visualized flow fields includes the motion of the wing, therefore the formation and shedding of the leading edge vortex. Consequently, the first two periods resembles for the upstream conditions, on the other hand, the last two periods the repetition is for both the upstream and downstream conditions. However, the same comment is not valid for the computational results. It is understandable why the first period of gust is very different since the fluctuations of gust starts with the motion and are not actually present there. Major features of the flow field are similar in both experimental and computational results for the period following the motion of the wing. The transverse velocity distributions during the formation (at $t=5s$) and shedding (at $t=6s$) of the leading edge vortex are similar especially in the near-wake, however afterwards as the gust cannot cause the formation and shedding of such large-scale structures, the similarity for the near-wake diminishes. The three-dimensionality of the flow at this time plays also an important role evident from the computational results for two different cross-sectional planes. At this point, it should be noted that the simulations are run for a wing of $AR=4$, while the experiments are performed for a wing of $AR=6$. Figure 6 shows on the lift force coefficient variations where the flow field snapshots are taken. The flow field results agree well with the force variations; the similarities during or just after the motion match and according to the force variations a diminishing phase is present between the computational and experimental results. Evidently, at $t=16s$ the flow fields also start to present same features especially in the near-wake in addition to the upstream conditions.

Figure 7 shows in detail what happens during the pitch up motion in terms of both streamline patterns combined with the vorticity distributions and the lift coefficient variation. In general, regarding the major features, experimental and computational results are in agreement. However, there are two differences between the two approaches. Although both approaches end up having transverse velocity fluctuations, those are created by periodic vortex gusts in the experiments. This is evident in the upstream vorticity distributions. The second difference is the extension of the leading edge vortex evident in both the streamline patterns and the vorticity contours. Probably, the vortex gust enhances the leading edge vortex for this encounter time, also in accordance with the force variation with respect to the case without gust.

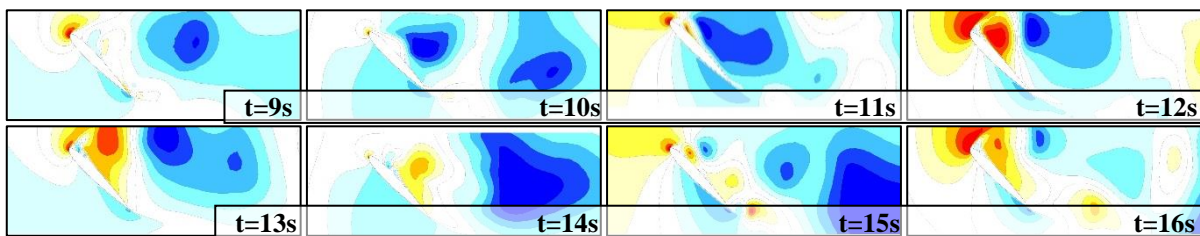
Figure 8 shows both streamline patterns combined with the vorticity distributions and the lift coefficient variation after the motion ends with 0.5s steps until one gust period is over from the beginning of the motion and 1s steps afterwards. Most of the flow features are also captured in agreement after the motion ends in both experimental and computational results. The aforementioned comments for the upstream is still valid; however, the near-wake exhibits other dissimilarities between the two approaches. Just after the motion ends, the flow structure positionings are very similar, but this time computational results yield stronger vorticity distributions. However, at $t=8s$, the leading edge vortex is already shed in the computational results while there is a lag introduced in the experimental results. The flow field observations are also in accordance with the loading; at $t=8s$, the lift coefficient starts to decrease in the computational results, however, it just reached its maximum in the experimental results. This timing difference between two approaches becomes more pronounced at later instants. On the other hand, as oppose to the observations made during the motion, the extension of vortex formations are greater for the computational approach, the experimental results show the occurrence of those flow structures closer to the wing surface. This is evident from the streamline topology, the arrows for $t=7s$ and $t=7.5s$ show the instantaneous location of the shed vortex, the circles for $t=9s$, $10s$ and $11s$ show the location of the saddle point which is a sign for the three-dimensionality effects. The force-time history also reflects those dissimilarities. On the other hands, based on Figure 4, a convergence between two approaches are also expected later, the lag seems to decrease towards the end of the simulations.



(a) Experimental



(b) computational at mid plane



(c) computational at the quarter span plane

Figure 5: Transverse velocity distributions during four periods of gust

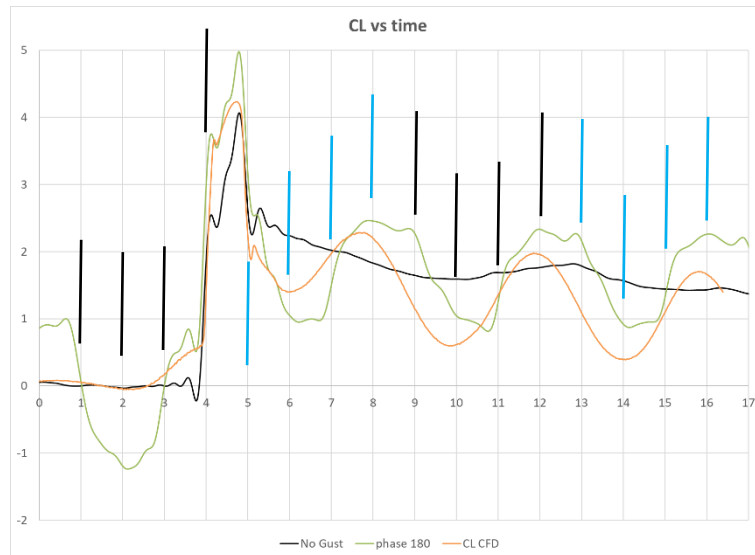


Figure 6: Lift coefficient variation with time showing where the transverse velocity distributions are taken

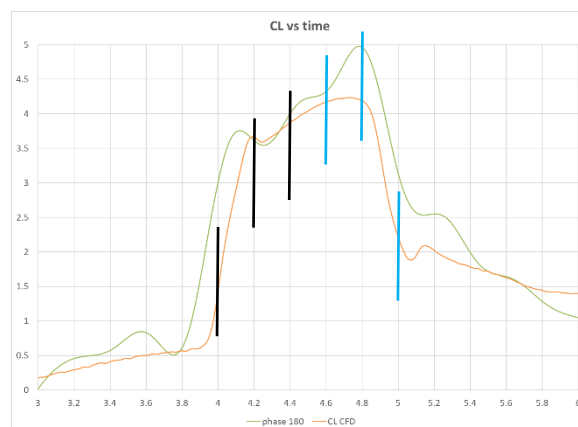
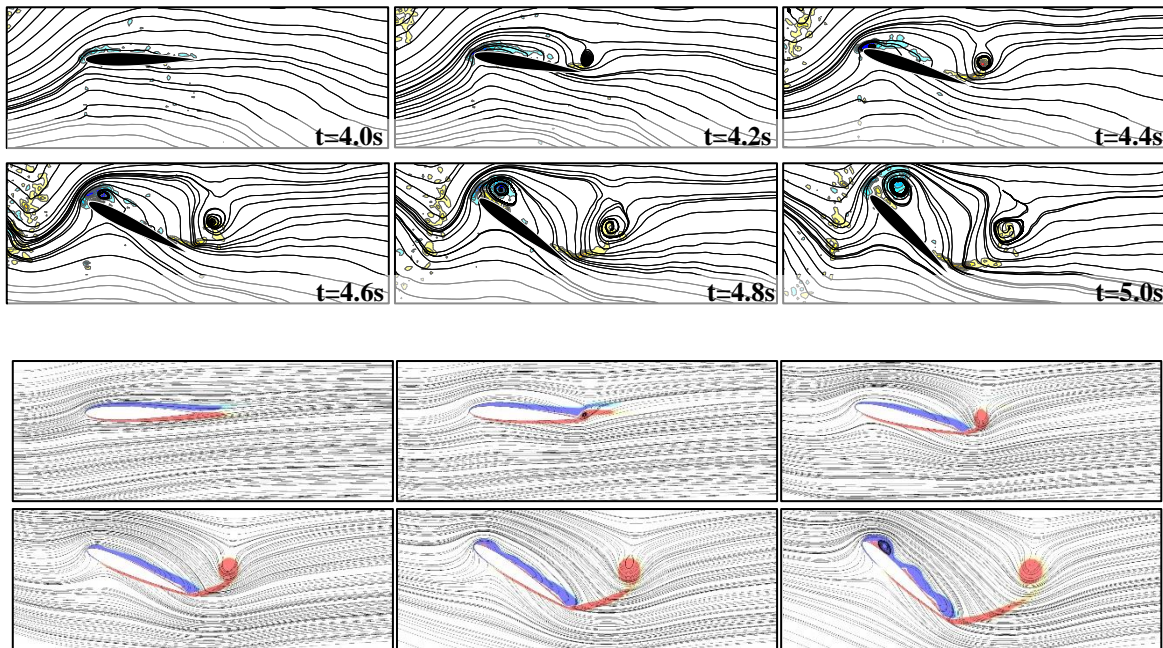


Figure 7: Streamline patterns combined with the vorticity distributions and the lift coefficient variation during the pitch-up motion

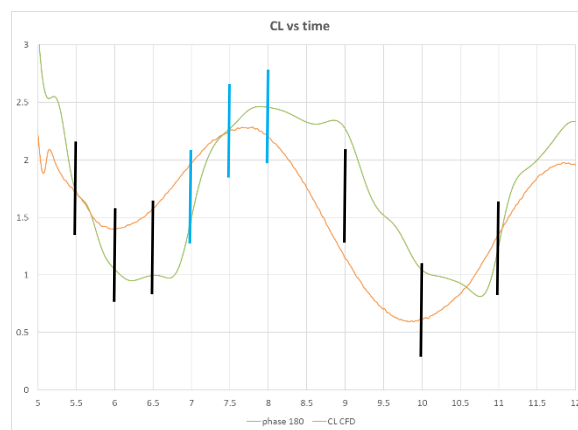
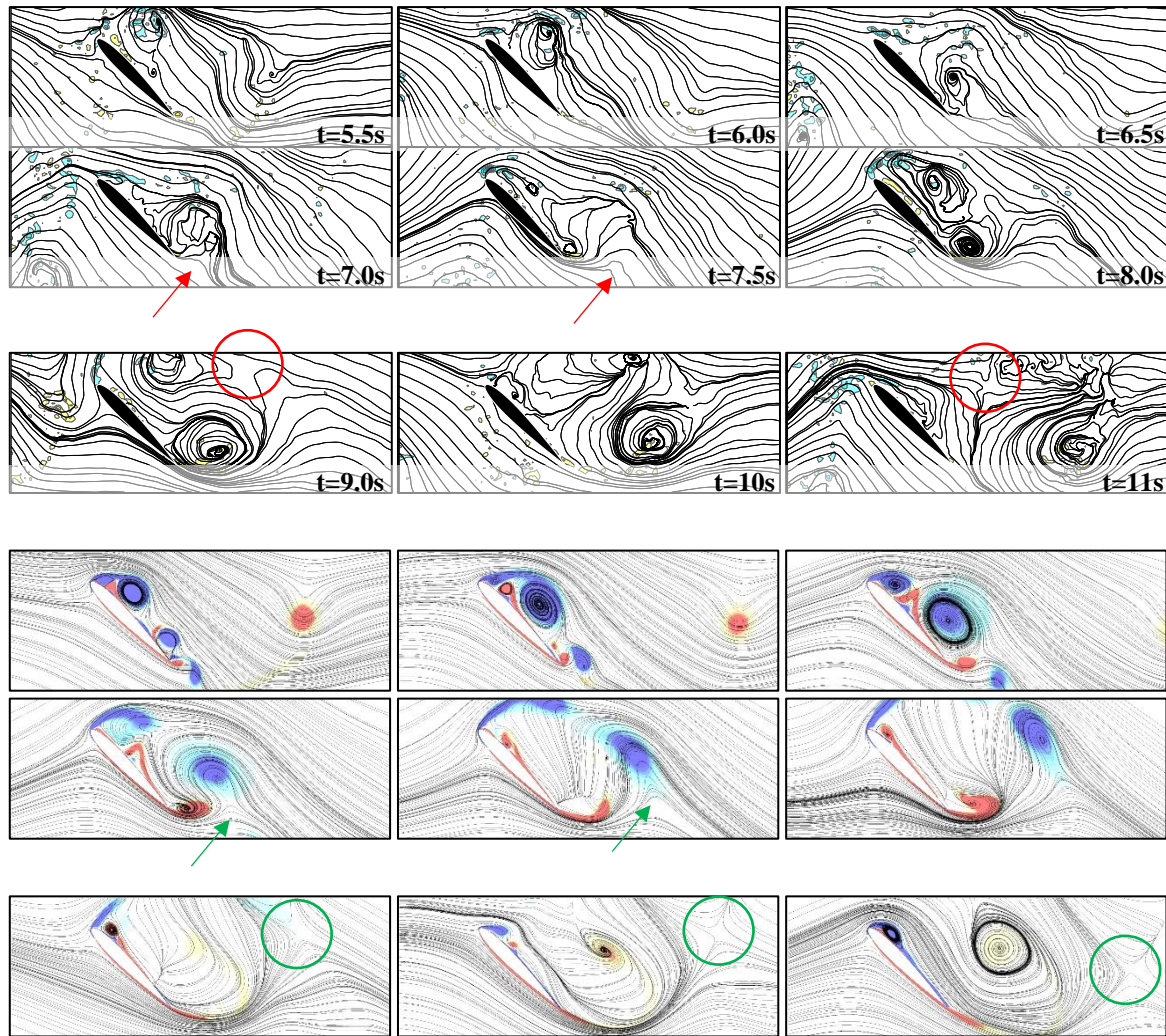


Figure 8: Streamline patterns combined with the vorticity distributions and the lift coefficient variation after the pitch-up motion

CONCLUSION

Two cases involving massive flow separation have been studied numerically in presence of a large scale spanwise gust. A NACA0012 wing has an aspect ratio of 4 and is either at an angle of attack of 45° or pitching up from zero to the same angle of attack in a uniform flow of $Re=10000$. The simulations consider periodic transverse velocity fluctuations while these fluctuations are obtained experimentally by periodic vortex shedding. Although both approaches consider the same pitch-up motion in 1 convective time, the aspect ratio of the

model in the experiments is 6. The gust encounter time is adjusted between two approaches, however the approach conditions are different. Despite all differences, the results agree well and the differences are found to be mostly related to the three-dimensionality effects. Although the sensitivity analyses are still studied and the simulations did not reach their final tuning, the investigation reached its goal and showed that such complex flow structure interaction problem at low speed can be simulated successfully. The simulations constitute an important tool for the understanding of the flow in detail three-dimensionally and resolved in time.

Acknowledgements

The experimental study is supported by TUBITAK Grant 115M358 (For the Application on UAVs and MAVs, Gust Effect on the Performance of Wings in Motion (Maneuver or Flapping) and Flow Control Attempts).

References

- Anderson, D. J. (1995), "Computational Fluid Dynamics: The basics with applications," McGraw Hill Inc.
- ANSYS® Fluent (2013a), Release 15.0, User's Guide, Ansys Inc.
- ANSYS® Fluent (2013b), Release 15.0, Theory Guide, Ansys Inc.
- Biler, H., Zaloglu, B. and Cetiner, O. (2015) Effect of Spanwise Gust on a Wing, 8th Ankara International Aerospace Conference, 10-12 September, METU, Ankara TURKEY.
- Comte-Ballot, G. and Corrsin, S. (1966), *The use of a contraction to improve the isotropy of grid generated turbulence*, Journal of Fluid Mechanics, 25(4), 657–682.
- Fisher, A.M. (2013), *The Effect of Freestream Turbulence on Fixed and Flapping Micro Air Vehicle Wings*, PhD thesis, RMIT University, Melbourne, Australia.
- Kang, H. S., Chester, S., and Meneveau, C. (2003), *Decaying turbulence in an active-grid-generated flow and comparisons with large-eddy simulation*, Journal of Fluid Mechanics, 480, 129–160.
- Lian, Y. and Shyy, W (2007), *Laminar-Turbulent Transition of a Low Reynolds Number Rigid or Flexible Airfoil*, AIAA Journal, 45(7), 1501–1513.
- Lian, Y. (2009), *Numerical Study of a Flapping Airfoil in Gusty Environments*, 27th AIAA Applied Aerodynamics Conference, San Antonio, TX.
- Milbank, J., Loxton, B., Watkins, S., and Melbourne, W. (2005), *Replication of Atmospheric Conditions for the Purpose of Testing MAVs*. Technical report, RMIT.
- Patankar, S.V. and Spalding, D.B. (1972), *A Calculation Procedure Heat, Mass and Momentum Transfer in Three-dimensional Parabolic Flows*, Int. J. Heat and Mass Transfer, Vol.15, pp. 1787-1806.
- Son, O. and Cetiner, O. (2017), *Three-Dimensionality Effects due to Change in the Aspect Ratio for the Flow around an Impulsively Pitching Flat Plate*, Journal of Aerospace Engineering, Vol. 30, Issue:5.
- Son, O., Cetiner, O., Stevens, P. R. R. J., Babinsky, H., Manar, F., Mancini, P., Jones, A.R., Ol, M.V. and Gozukara, A.C. (2016), *Parametric Variations in Aspect Ratio, Leading Edge and Planform Shapes for the Rectilinear Pitch Cases of AVT-202 (Invited)*, 54th AIAA Aerospace Sciences Meeting, AIAA-2016-0289 (<http://dx.doi.org/10.2514/6.2016-0289>), 4-8 January 2016, San Diego, California, USA.
- Stevens, P. R. R. J., Babinsky, H., Manar, F., Mancini, P., Jones, A.R., Granlund K.O., Ol, M.V. Nakata T., Phillips N., Bomphrey R.J. and Gozukara, A.C. (2016), *Low Reynolds Number Acceleration of Flat Plate Wings at High Incidence, (Invited)*, 54th AIAA Aerospace Sciences

Meeting, AIAA-2016-0286 (<http://dx.doi.org/10.2514/6.2016-0286>), 4-8 January 2016, San Diego, California, USA.

Watkins, S., Milbank, J., Loxton, B. J., Melbourne, W. H., (2006), *Atmospheric winds and their implications for microair vehicles*, AIAA Journal, 44(11), 2591-2600.